

PAPER • OPEN ACCESS

On the microstructure evolution of a nuclear-use steel after heavy ion irradiation

To cite this article: Ligang Song *et al* 2021 *IOP Conf. Ser.: Earth Environ. Sci.* **639** 012013

View the [article online](#) for updates and enhancements.

You may also like

- [Damage effects of Au&He dual ion irradiated silicon carbide](#)
Xu Wang, Ziqiang Zhao, Ming Zhang *et al.*
- [Structural health monitoring feature design by genetic programming](#)
Dustin Y Harvey and Michael D Todd
- [Defect recovery and damage reduction in borosilicate glasses under double ion beam irradiation](#)
A. H. Mir, S. Peugnet, M. Toulemonde *et al.*



The Electrochemical Society
Advancing solid state & electrochemical science & technology

241st ECS Meeting

May 29 – June 2, 2022 Vancouver • BC • Canada

Extended abstract submission deadline: Dec 17, 2021

Connect. Engage. Champion. Empower. Accelerate.
Move science forward



Submit your abstract



On the microstructure evolution of a nuclear-use steel after heavy ion irradiation

Ligang Song¹, Fan Ye¹, Jianghua Li², Xianfeng Ma^{1*}, Ruiqian Zhang^{3*}, Shui Qiu³, Xiao Liu³

¹Sino-French Institute of Nuclear Engineering and Technology, Sun Yat-Sen University, Zhuhai 519082, Guangdong, China

²State Key Laboratory of Nonlinear Mechanics (LNM), Institute of Mechanics, Chinese Academy of Sciences, Beijing 100190, China

³Science and Technology on Reactor Fuel and Materials Laboratory, Nuclear Power Institute of China, Chengdu, Sichuan 610041, China

* Corresponding author's e-mail: maxf6@mail.sysu.edu.cn (X. Ma); zhang_ruiqian@126.com (R. Zhang).

Abstract. A nuclear-use ferritic-martensitic steel was irradiated by 196 MeV Kr ions. Both the low damage level area and the high damage level area were investigated by a transmission electron microscope (TEM), to reveal the irradiated microstructural features. In low damage level area ranging from surface to 6 μm depth, there were a few dislocation loops and black dots induced by Kr irradiation. The type of dislocation loops could be primarily $a_0\langle 100 \rangle$ or $a_0/2\langle 100 \rangle$ type. In addition, it was found that the sink effect of grain boundaries and stability of small precipitates were evident.

1. Introduction

Ferritic-martensitic (F/M) steels have a number of attractive properties for use as cladding and ducts in reactors, including high strength at elevated temperatures, good compatibility and excellent swelling resistance under irradiation [1-3]. At reactor operating temperatures, irradiation creep becomes a major concern. An understanding of the microstructure evolution was required to determine the suitability of these steels for the intended application. The majority of the recent efforts had been focusing on the microstructure evolution during irradiation in reactors operating condition [4, 5]. However, neutron irradiation was too expensive and time consuming to explore comprehensively the evolution of microstructure. The ions implantation provides an effective way to induce irradiation damage to simulate the neutron irradiation [6]. Besides, heavy ions implantation can operate at controlled temperature. By ions implantation, phase stability of precipitates in ferritic-martensitic steel T91 under proton irradiation was investigated [7, 8]. Heavy ions irradiation like Fe ions was used to study pre-existing precipitates and induce formation of needle-like M_3C particles [9]. Ultra high damage levels can also be realized and it was found that swelling was accompanied by radiation-induced precipitation of Cu-rich and Si, Ni, Mn-rich phases [10]. There are many other studies on variable microstructure by utilizing ions implantation [11] at different irradiation condition such as temperature, dual beam ions irradiation. In this study, to provide additional insight into the microstructure evolution of FM steels [12] at high temperature, experiments were conducted using 196 MeV Kr ions at 550 °C.



2. Experiments details

The chemical composition of a ferritic-martensitic steel T91 used in this study is listed in Table 1. The T91 steel was normalized at 1045 °C for 10 mins, followed by air cooling, and then tempered at 780 °C for 1 hour followed by air cooling. A 10×10×1 mm T91 sample was cut by electrical discharge machining. The sample was mechanically polished with silicon carbide papers, and then electropolished using 10% perchloric acid and 90% ethyl alcohol.

Table 1. The chemical composition (wt%) of original T91 steel

Fe	Cr	C	Mn	Mo	Nb	Al	Cu	V	Si	Ni	S	P
Bal.	8.53	0.1	0.4	0.15	0.076	0.01	0.022	0.21	0.38	0.12	0.001	0.015

The polished specimen was irradiated by 196 MeV Kr ions at 550 °C. Two sets of magnets were used to scan the ion beam with an area of 15×15 mm² during the ion beam bombarding on the specimen to obtain a relatively uniform distribution in the radiation dose.

By SRIM-2008 Kinchin-Pease quick calculation [11] shown in Figure 1, Kr concentration distribution is over 10 to 12 μm damage depth from surface. The damage peak position is located at ~ 11 μm depth from surface and the value of peak damage is about 30 displacement per atom (dpa). Below the depth of 10 μm, the ratio of Kr concentration to dpa is nearly zero. It indicates that there is no significant effect of Kr atoms range from surface to 10 μm. In order to avoid the effect of impurity atoms, we mainly focused on the microstructure evolution of Kr-irradiated T91 steel below the depth of 10 μm.

3. Method of analysis

Transmission Electron Microscope (TEM) analyses were carried out on an FEI Talos 200X TEM microscope to study the damage accumulation after irradiation. The TEM samples were fabricated by focused ion beam (FIB) lift-out technique with a FEI Quanta 3D FEG dual beam scanning electron microscopy (SEM). The length of original T91 samples reached 4 μm. The length of Kr-irradiated T91 samples reached 12 μm, completely including the irradiation depth. In order to reduce contingent artifacts and obtain fine surface on FIB cross-section plane, a platinum (Pt) layer was deposited to protect the surface from ion damaging, and then the sample was milled from both sides to the final thickness of approximately 55 nm with the lowest possible current beam.

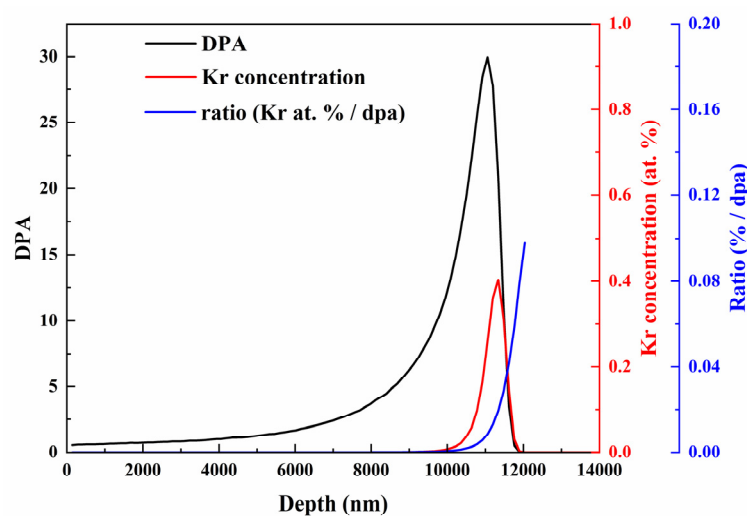


Figure 1. The damage level, Kr concentration and ratio of concentration to dpa in Kr-irradiated T91 sample simulated by SRIM-2008

4. Results and discussion

In Figure 2, it was found that there were much low density dislocations in the bright filed image of original T91 sample. In corresponding dark field image, there is rarely defects existed in original sample. Some precipitates such as usually carbides like $M_{23}C_6$ [13] ranged from 40~200 nm were distributed along the grain or sub-grain boundaries.

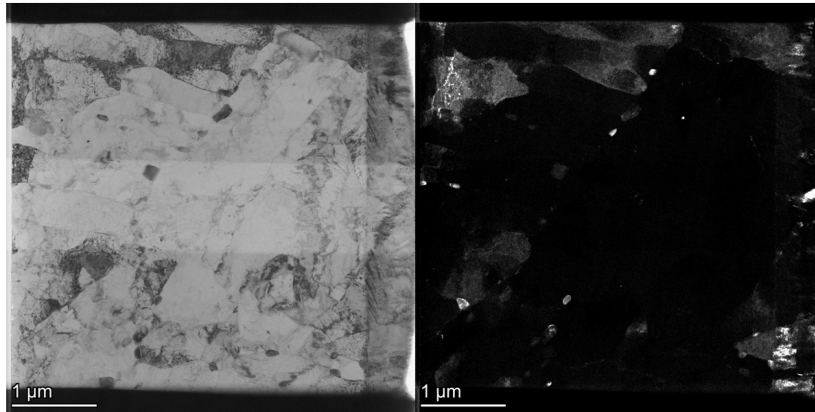


Figure 2. TEM bright and dark field images of original T91 sample fabricated by FIB

In Figure 3 and Figure 4, it was shown that the density of defects increased in Kr-irradiated T91 sample, as shown in Figure 3 and Figure 4. Within depth of 6 μm , the damage level is lower than 3 dpa, but it was also possible to induce dislocation loops by irradiation [6]. Interestingly, there is much more dislocation loops produced by irradiation in some grains close to surface than other grains in deep layer. But the grain boundaries existed in the depth from surface to 3 μm are more distinguished than that in the depth from 3 to 6 μm . From Figure 1, the damage level of 3 μm and 6 μm deep layer are 0.84 dpa and 1.68 dpa, respectively. With increasing of damage level, more dislocation loops or vacancies produced by irradiation would migrate to grain boundaries and dislocations pile up near the grain boundaries, which would make the grain boundaries amorphous or indistinguishable.

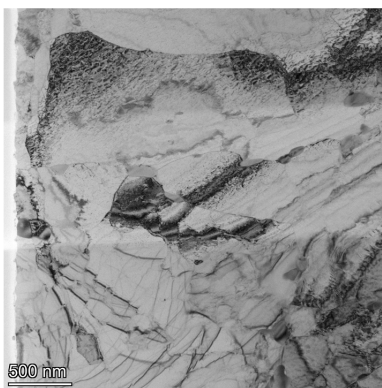


Figure 3. TEM image ranges from surface to 3 μm depth in Kr irradiated-T91 sample.

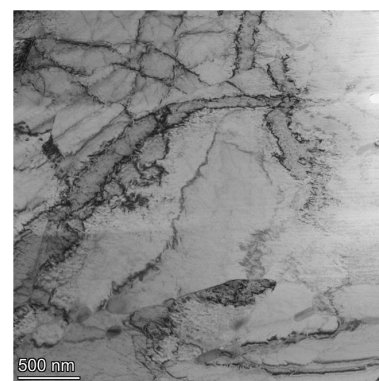


Figure 4. TEM image ranges from 3 to 6 μm depth in Kr irradiated-T91 sample.

The area in the depth of $\sim 1 \mu\text{m}$ was selected to apply the electron diffraction. The corresponding TEM images and FFT diffraction patterns of T91 sample were show in Figure 5. The diffraction pattern indicated a typical BCC crystal structure.

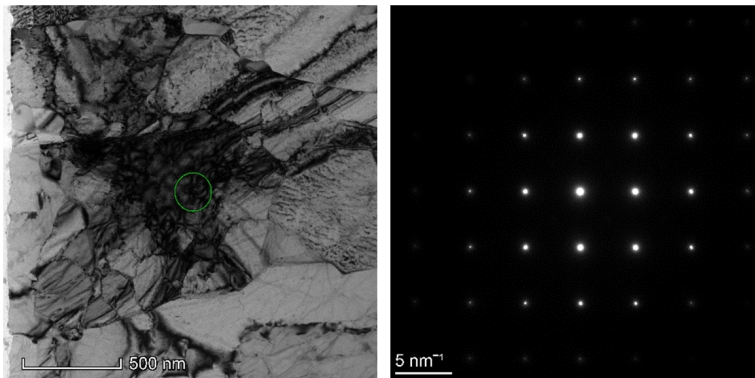


Figure 5. TEM image and FFT diffraction pattern of T91 sample irradiated by Kr ions and the depth of diffraction area is lower than 6 μm .

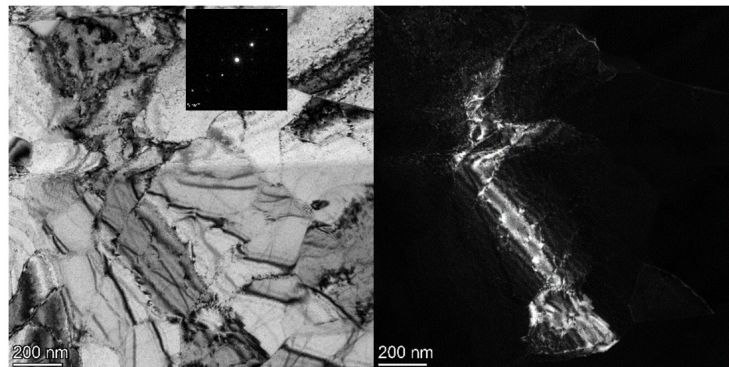


Figure 6. TEM bright and dark field images from surface to 6 μm depth of T91 sample irradiated by Kr ions under the diffraction vector $g=200$

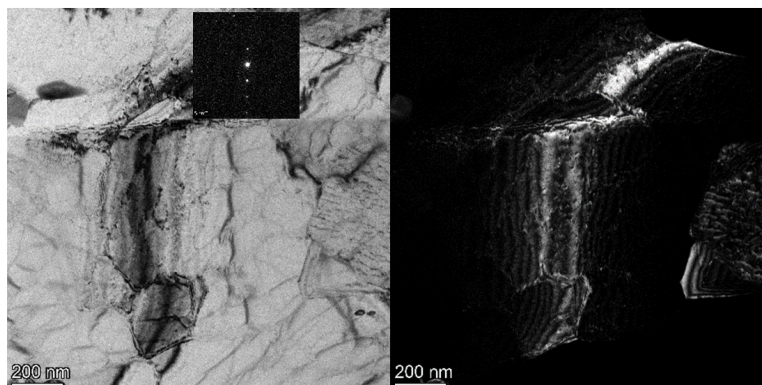


Figure 7. TEM bright and dark field images from surface to 6 μm depth of T91 sample irradiated by Kr ions under the diffraction vector $g=1-10$

In Figure 6, the TEM bright and dark field images within from surface to 6 μm depth of Kr-irradiated T91 under the diffraction vector $g=200$ has shown that low density dislocation loops or black dots were produced. Generally, the contrast of dislocation loops is expected to vanish or become faint under diffraction condition while $g \cdot b = 0$. The Burgers vector of dislocation loops can be determined by the $g \cdot b$ analysis under variable diffraction vector. Therefore, according to the TEM bright and dark field images in the same area under the diffraction vector $g=1-10$, as shown in Figure 7, the type of vectors

of dislocation loops produced by irradiation in Kr-irradiated T91 samples were believed as $a_0\langle 100 \rangle$ or $a_0/2\langle 100 \rangle$ type [3, 14]. It was noticeable that there were small size precipitates in Figure 3 and 4 within low damage area. It could indicate that some small precipitates would be less affected by irradiation, which is similar to other study [9].

5. Conclusion

A ferritic-martensitic steel for nuclear reactor use was irradiated by high-energy heavy ions of 196 MeV Kr at 550 °C. The microstructures before and after irradiation were investigated under Transmission Electron Microscope. In the low damage area, there were only a few dislocation loops and black dots. The type of dislocation loops were identified as $a_0\langle 100 \rangle$ or $a_0/2\langle 100 \rangle$ type. In addition, the sink effects of grain boundaries and the stability of small precipitates were found in the Kr-irradiated T91 steels.

Acknowledgement

This project is supported by the STRFML-2018-25 Fund of the Science and Technology on Reactor Fuel and Materials Laboratory, Nuclear Power Institute of China. The authors also acknowledge the support from the National Science Foundation of China (No. U2032143, 11902370, 52005523), Guangdong Major Project of Basic and Applied Basic Research (2019B030302011), International Sci & Tech Cooperation Program of Guangdong Province (2019A050510022), Key-Area Research and Development Program of Guangdong Province (2019B010943001, 2017B020235001), China Postdoctoral Science Foundation (2019M653173 and 2019TQ0374), Guangdong Education Department Fund (2016KQNCX005), and Fundamental Research Funds for the Central Universities (19lgpy304).

References

- [1] C. Heintze, F. Bergner, S. Akhmadaliev, E. Altstadt, Ion irradiation combined with nanoindentation as a screening test procedure for irradiation hardening, *Journal of Nuclear Materials* 472 (2016) 196-205.
- [2] H.P. Zhu, Z.L. Hao, T.L. Shen, M.H. Cui, X.S. Fang, Z.G. Wang, F.L. Niu, Y.G. Zhao, A.X. Yang, Y. Zhang, Evolution of vacancy-type defects and hardening behaviors of T91 induced by 1.625 MeV Fe-ions at different temperatures, *Fusion Eng Des* 125 (2017) 372-377.
- [3] Z. Jiao, S. Taller, K. Field, G. Yeli, M.P. Moody, G.S. Was, Microstructure evolution of T91 irradiated in the BOR60 fast reactor, *Journal of Nuclear Materials* 504 (2018) 122-134.
- [4] Z.X. Shang, J. Ding, C.C. Fan, D. Chen, J. Li, Y.F. Zhang, Y.Q. Wang, H.Y. Wang, X.H. Zhang, He ion irradiation response of a gradient T91 steel, *Acta Materialia* 196 (2020) 175-190.
- [5] C. Zheng, D. Kaoumi, Dislocation loop evolution in F/M steel T91 under in-situ ion irradiation: Influence of the presence of initial dislocations, *Journal of Nuclear Materials* 540 (2020).
- [6] W. Van Renterghem, D. Terentyev, M.J. Konstantinovic, Transmission electron analysis of dislocation loops in T91 steels from MEGAPIE and MIRE irradiation experiments, *Journal of Nuclear Materials* 506 (2018) 43-52.
- [7] Z.J. Jiao, V. Shankar, G.S. Was, Phase stability in proton and heavy ion irradiated ferritic-martensitic alloys, *Journal of Nuclear Materials* 419(1-3) (2011) 52-62.
- [8] E. Getto, K. Sun, A.M. Monterrosa, Z. Jiao, M.J. Hackett, G.S. Was, Void swelling and microstructure evolution at very high damage level in self-ion irradiated ferritic-martensitic steels, *Journal of Nuclear Materials* 480 (2016) 159-176.
- [9] C.C. Wei, A. Aitkaliyeva, M.S. Martin, D. Chen, L. Shao, Microstructural changes of T-91 alloy irradiated by Fe self ions to ultrahigh displacement ratios, *Nucl. Instrum. Methods Phys. Res. Sect. B-Beam Interact. Mater. Atoms* 307 (2013) 181-184.
- [10] J.G. Gigax, T. Chen, H. Kim, J. Wang, L.M. Price, E. Aydogan, S.A. Maloy, D.K. Schreiber, M.B. Toloczko, F.A. Garner, L. Shao, Radiation response of alloy T91 at damage levels up to 1000 peak dpa, *Journal of Nuclear Materials* 482 (2016) 257-265.
- [11] J.P. Biersack, J.F.J.I.I.e. Ziegler, *Technology, The Stopping and Range of Ions in Solids*, 1(1) (1984)

51-108.

- [12] P. Van Houtte, S.Y. Li, M. Seefeldt, L. Delannay, Deformation texture prediction: from the Taylor model to the advanced Lamel model, *Int. J. Plasticity* 21(3) (2005) 589-624.
- [13] L. Tan, B.K. Kim, Y. Yang, K.G. Field, S. Gray, M. Li, Microstructural evolution of neutron-irradiated T91 and NF616 to similar to 4.3 dpa at 469 degrees C, *Journal of Nuclear Materials* 493 (2017) 12-20.
- [14] X. Liu, Y.B. Miao, M.M. Li, M.A. Kirk, S.A. Maloy, J.F. Stubbins, Ion-irradiation-induced microstructural modifications in ferritic/martensitic steel T91, *Journal of Nuclear Materials* 490 (2017) 305-316.